Available online at www.sciencedirect.com

ScienceDirect

journal homepage: www.jfda-online.com

Review Article

Theranostic nanomedicine for cancer detection and treatment☆

Zhen Fan [a], *Peter P. Fu* [b], *Hongtao Yu* [a], *Paresh C. Ray* [a,*]

[a] *Department of Chemistry and Biochemistry, Jackson State University, 1400 J.R. Lynch St, Jackson, MS, USA*
[b] *Division of Biochemical Toxicology, National Center for Toxicological Research, Food and Drug Administration, 3900 NCTR Road, Jefferson, AR, USA*

ARTICLE INFO

Article history:
Received 30 September 2013
Received in revised form
18 December 2013
Accepted 24 December 2013
Available online 31 January 2014

Keywords:
Circulating tumor cell diagnosis
Combined therapy
Photothermal therapy
Selective cancer treatment
Theranostic nanomedicine

ABSTRACT

Cancer is the second leading cause of death in the USA according to the American Cancer Society. In the past 5 years, "theranostic nanomedicine", for both therapeutics and imaging, has shown to be "the right drug for the right patient at the right moment" to manage deadly cancers. This review article presents an overview of recent developments, mainly from the authors' laboratories, along with potential medical applications for theranostic nanomedicine including basic concepts and critical properties. Finally, we outline the future research direction and possible challenges for theranostic nanomedicine research.

1. Introduction

According to the American Cancer Society, approximately 1,660,290 new cancer cases are expected to be diagnosed in 2013 [1]. The American Cancer Society also projects that 580,350 will die from cancers in 2013, and cancer will account for almost 1 in every 4 deaths. Early detection and effective treatment of cancer is the key to saving lives. It is well documented that the major cause of cancer mortality is tumor metastasis [2–10]. Because cancer cell dissemination mostly occurs through the bloodstream via circulating tumor cells (CTCs), scientists and medical professionals have been working to develop new approaches for early stage detection of CTCs to help physicians treat patients and predict cancer progression [11–25]. Although CTCs have been known since 1869, they can only be detected in patients with advanced stage tumors [26–40]. Because CTCs are present at extremely low levels, accounting for only a few cells/10^6 peripheral blood mononuclear cells, it is a challenge for early detection. To overcome this problem, effective separation and enrichment is highly crucial [22–24,39,41–56]. Recent reports show that use of nanomaterials as contrast agents and therapeutic actuators is one of the most promising methods, although this is still at an infant stage [25,26,28,34,35,37,40,42,48,49,51,57–66]. Because nanoparticles exhibit unique optical, magnetic, and

☆ This article is not an official FDA guidance or policy statement. No official support or endorsement by the FDA is intended or should be inferred.

* *Corresponding author*. Department of Chemistry and Biochemistry, Jackson State University, Jackson, MS 39217, USA.
E-mail address: paresh.c.ray@jsums.edu (P.C. Ray).

http://dx.doi.org/10.1016/j.jfda.2014.01.001

photothermal properties, they can be exploited for selective detection as well as noninvasive photothermal therapy of cancer [10–30]. During the past 5 years, it has been shown that diagnosis and therapy can be combined within a single multifunctional nanomaterial, known as "theranostic nanoparticles" [10–30]. The ideal theranostic nanomaterial should possess several advantages [10–35]: (1) the ability for highly selective accumulation in the diseased tissue, (2) capable of delivering an effective therapeutic action selectively, and (3) safe and can undergo biodegradation into nontoxic byproducts. We believe that development of effective theranostic materials is one of the keys for detection and treatment of early stage cancer in the 21st century. In this review, we will highlight recent advances in the development of "theranostic nanomedicine" mainly from the authors' research. We will also speculate on the future of research and technological applications on theranostic nanomedicine.

2. Theranostic nanomedicine

During the past decade, it has been demonstrated [5–20] that nanoparticles of 4–100 nm, which are 1000–10,000 times smaller than normal human cells, exhibit strong interactions with biomolecules such as enzymes, receptors and antibodies, both on the surface and inside the cell. By surface chemical modification, nanoparticles can be coated, functionalized, and integrated with a variety of bioconjugated moieties for selective detection and treatment [22–40]. Thus, we believe nanomedicine will lead breakthroughs for detection, diagnosis, and treatment of cancer. Recent advances in nanoscience allow us to design and place three functions, namely targeting, diagnosis, and therapeutics, into one nanomedicine [66–77]. Theranostic nanomedicine is based on this concept of combining both therapeutic and diagnostic functions into one nanoparticle, as shown in Fig. 1.

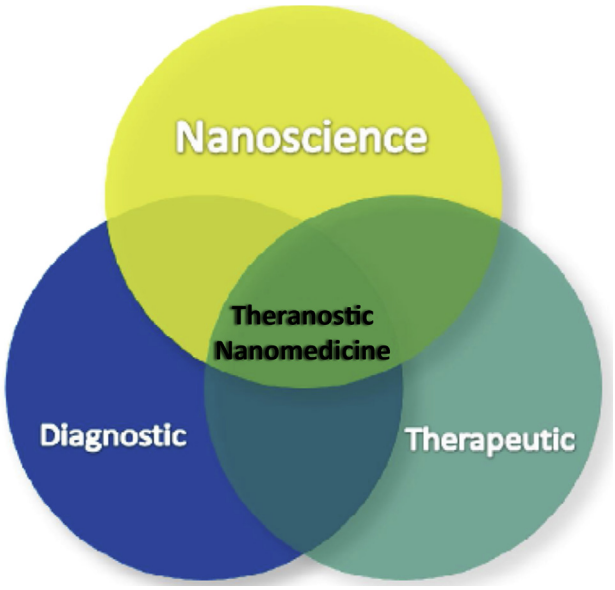

Fig. 1 – Scheme illustrating the combination of both therapeutic and diagnostic functions into theranostic nanomedicine.

3. Theranostic toolbox for CTC detection

Some tumor cells are continuously shed from a primary tumor site into the vasculature to circulate in the blood system. These are named CTCs, and are believed to account for the growth and spread of metastasis tumors and to be responsible for the majority of cancer-related deaths [2–10]. CTCs were first observed in 1869 from the blood sample of a male metastatic cancer patient by Thomas Ashworth, who assumed that "cells identical with those of the cancer itself being seen in the blood may tend to throw some light upon the mode of origin of multiple tumors existing in the same person" [10–20]. Due to the ease of obtaining blood samples, detection of extremely low concentrations of CTCs will lead to effective and minimally invasive early stage diagnosis of cancer, as well as to predict responses to therapy of patients with metastatic cancers [10–20]. Despite the clinical importance of CTCs, the isolation and enrichment of CTCs from whole blood remains a challenge due to their extremely low concentrations in blood [21–30].

To tackle this challenge, we have developed a multifunctional plasmonic shell-magnetic core nanotechnology-driven approach for targeted diagnosis and isolation of cancer cells [15,16]. Because noble metal nanoparticles exhibit unique and versatile optical properties, there is a wide variety of contrast mechanisms for cell optical imaging [21–30]. Plasmonic gold nanoparticles have been widely used as agents for detection and targeting [31–40]. Through the enhanced second harmonic signal by antibody conjugated gold nanoparticles, cellular imaging of single molecules has been reported [17]. For example, iron oxide magnetic nanoparticles have been used as a contrast agent in magnetic resonance imaging and biological separation [10–20]. As a result, the integration of magnetic and plasmonic functions into a single platform with a magnetic core and a plasmonic shell should be hugely beneficial for early stage CTC detection [15,16]. Plasmonic gold coating on magnetic nanoparticles is very useful for stabilizing high-magnetic-moment nanoparticles under corrosive biological conditions. It will also allow easy bioconjugation through the well-understood chemistry of gold sulfide [15,16].

Magnetic core nanoparticles were synthesized by coprecipitation of Fe(II) and Fe(III) chlorides with 1.5 M NaOH as reported recently [15,16]. Gold shells were formed by reduction of Au^{3+} on the surface of iron oxide core (Fig. 2A). For magnetic separation of cancer cells followed by fluorescence imaging, the magnetic/plasmonic nanoparticles surface was modified with a cancer targeting aptamer. As shown in Fig. 2A, cyanine 3 (Cy3) modified S6 aptamers (specific targeting for the SK-BR-3 cell line via HER25) were attached to magnetic/plasmonic nanoparticles through –SH linkage. As reported previously [15,16], the plasmonic shell was functionalized with aptamer-modified Cy3 for: (1) specific breast cancer cell recognition via the aptamers; and (2) fluorescent imaging using Cy3 as the fluorescence probe. As shown in Fig. 2B, the magnetic core was used for cell isolation. Specific cancer cell imaging and separation for the human breast cancer cell line was based on

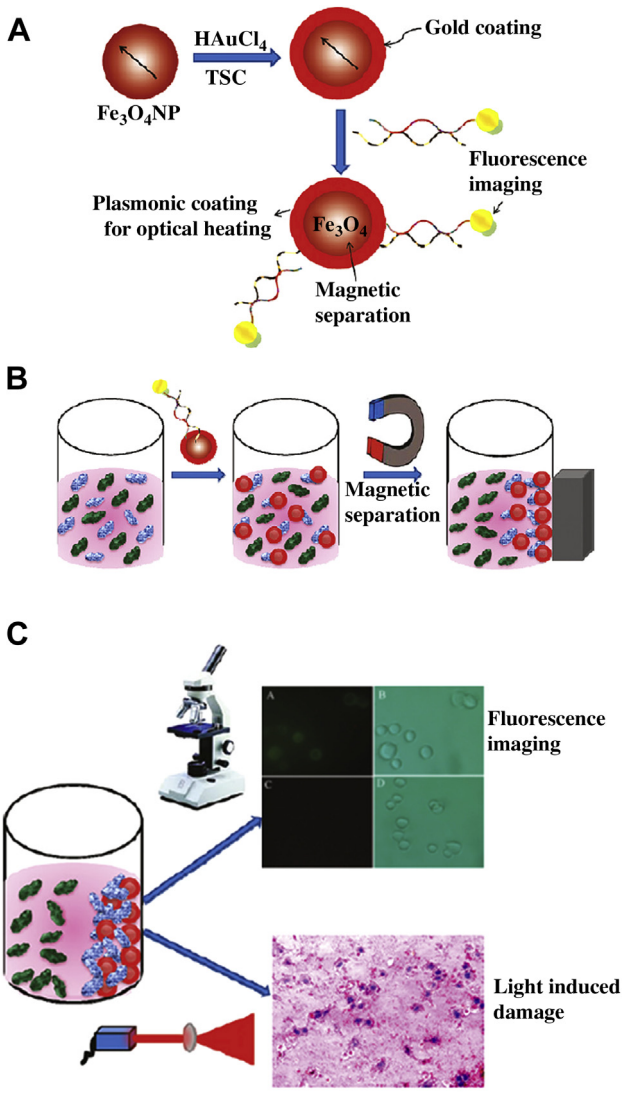

Fig. 2 – (A) Schematic representation showing synthesis of S6 aptamer-conjugated multifunctional magnetic core-gold shell nanoparticles. (B) Separation of specific cancer cells using S6 aptamer-conjugated plasmonic/magnetic nanoparticles. (C) Selective fluorescence imaging and targeted photothermal destruction of specific cancer cells. *Note.* From "Multifunctional plasmonic shell–magnetic core nanoparticles for targeted diagnostics, isolation, and photothermal destruction of tumor cells", by Z. Fan, M. Shelton, A.K. Singh, et al, 2012, *ACS Nano*, 6, p. 1065–73. Copyright 2012, *American Chemical Society*. Reprinted with permission.

that, in the presence of the SK-BR-3 cell line, S6 aptamer-conjugated magnetic/plasmonic nanoparticles attach to cancer cells (Figs. 2C and 3) due to the S6 aptamer-cancer cell interaction. To demonstrate the separation capability of very low concentrations of cancerous cells (0.001%), 100 μL of S6 aptamer-conjugated magnetic/plasmonic nanoparticles with 1 mL of human epidermal growth factor receptor 2 (HER2)-positive human SK-BR-3 breast cancer cell suspension containing 100 cells/mL and 1 mL of HER2-negative human skin cell HaCaT cell suspension containing 10^7 cells/mL were incubated together. After 120 minutes of incubation at room temperature under gentle shaking, the suspensions were washed to remove unconjugated Cy3-bound magnetic/plasmonic nanoparticles. Then the cancer cells were separated from the suspension using a small magnet. Confocal fluorescence imaging was taken after magnetic separation (Fig. 3). The imaging and separation of breast cancer cells from normal cells can be achieved in 0.001% mixtures.

In addition, we have recently reported a targeted isolation and detection of rare tumor cells from a whole blood sample through a theranostic plasmonic shell-magnetic core star shaped nanomaterial [16]. The theranostic core-shell star shaped gold nanoparticles were synthesized through a two-step process [16]. In the first step, very small spherical iron nanoparticles were synthesized using trisodium citrate as a stabilizer and sodium borohydride as a reducing agent [16]. In the second step, star shaped magnetic nanoparticles were synthesized using seed-mediated growth procedure in the presence of cetyltrimethylammonium bromide [16]. Next, to avoid nonspecific interactions with blood cells, star shaped magnetic/plasmonic nanoparticles were coated by thiolated polyethylene glycol (PEG) and then functionalized with an aptamer. As shown in Fig. 4, the magnetic core was used for cell isolation and enrichment. Cy3-modified S6 aptamers were attached to magnetic/plasmonic theranostic nanoparticles through –SH linkage for: (1) specific SK-BR-3 breast cancer cell recognition via the S6 aptamers; and (2) fluorescence imaging using Cy3 as the fluorescence probe [16]. Due to surface roughness, the star shaped magnetic-plasmonic particles can enhance protein corona attachment, which can enhance cellular uptake and magnetic separation capability.

The working principle for specific cancer cell separation from whole blood sample is based on the fact that, in the presence of the SK-BR-3 cell line, S6 aptamer-conjugated theranostic nanoparticles were attached to the cancer cells due to the S6 aptamer–cancer cell interaction [16], as shown in Fig. 5. To demonstrate the CTC separation from whole blood samples, 0.001% SK-BR-3 human breast cancer cells were spiked into the suspensions of citrated whole rabbit blood samples. After 120 minutes' incubation at room temperature under gentle shaking, cells attached with magnetic/plasmonic nanoparticles were separated by a magnet (Fig. 5). Then cells were diagnosed using fluorescence imaging (Fig. 5). Based on these results, it is believed that the theranostic nanoparticles can be used for imaging and separation of CTCs from the whole blood sample even at 0.001% cell mixtures.

Detection of CTCs is not only based on positive enrichment, but also a negative enrichment of CTCs using a geometrically activated surface interaction chip as reported by Hyun et al [21]. The geometrically activated surface interaction (GASI) chip with an asymmetric herringbone structure is designed to generate enhanced mixing flows [21] to increase the surface interaction between the nontarget cells and the channel surface. After that, CD45 antibodies are immobilized inside the channel to capture leukocytes and release CTCs to the outlet. The report [21] shows that the GASI chip using a herringbone shape can efficiently capture a large number of hematological cells rather than CTCs (Fig. 6A). The herringbone structure is patterned on the channel to produce

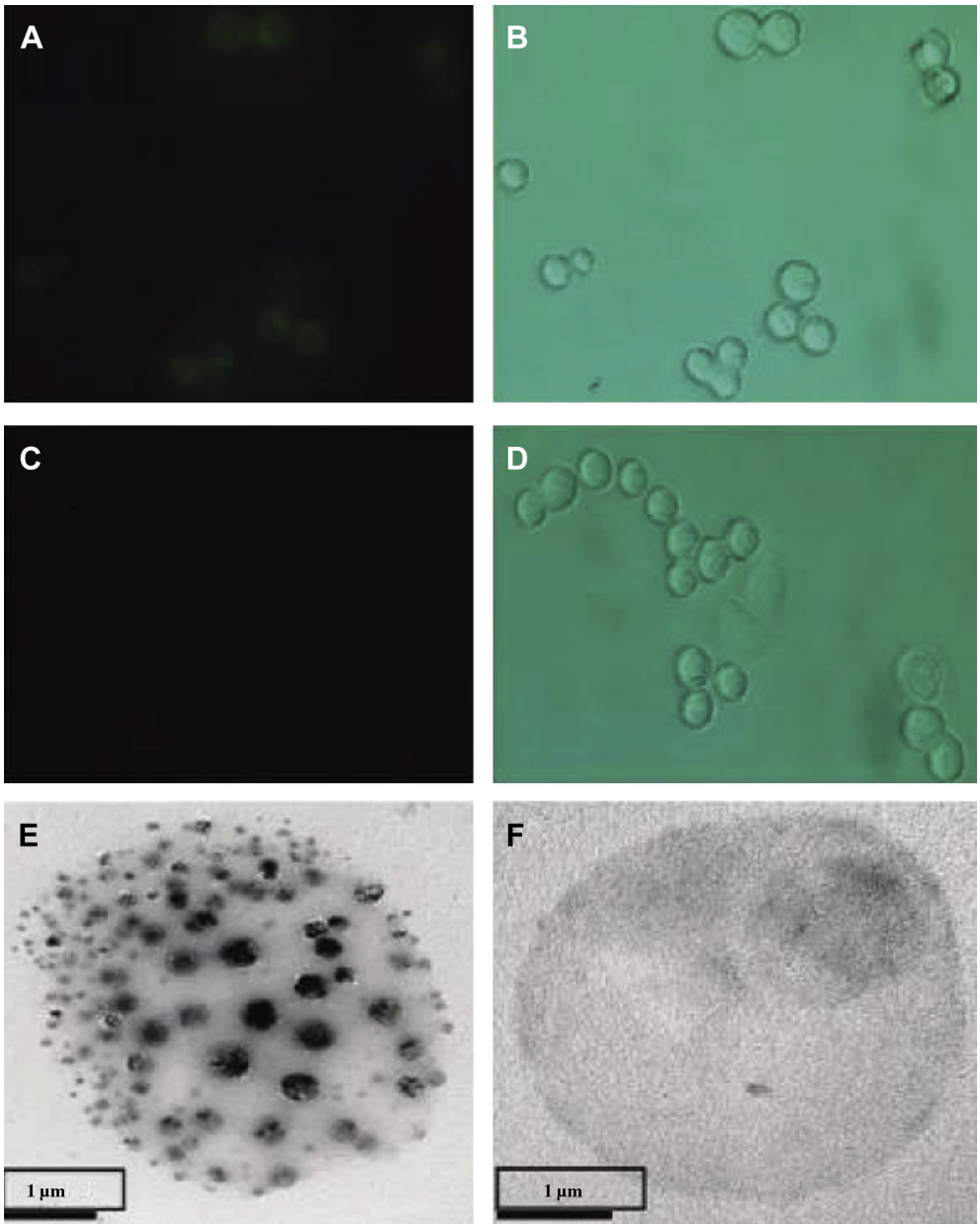

Fig. 3 – (A) Fluorescent images of SK-BR-3 cancer cells after a mixture of LNCaP and SK-BR-3 cells (1:10^{-4} ratio) was incubated with Cy3-modified S6 aptamer-conjugated magnetic/plasmonic nanoparticles and separated by a magnet. (B) Bright-field image of the same SK-BR-3 cells after magnetic separation. (C) LNCaP cancer cell fluorescent images after a mixture of LNCaP and SK-BR-3 cells (1:10^{-4}) was incubated with Cy3-modified S6 aptamer-conjugated magnetic/plasmonic nanoparticles and separated by a magnet. (D) Bright-field image of the same LNCaP cells after magnetic separation. (E) Transmission electron microscopy image of SK-BR-3 cells after magnetic separation. It clearly shows that Cy3-modified S6 aptamer-conjugated magnetic/plasmonic nanoparticles are attached to SK-BR-3 cells. (F) Transmission electron microscopy image of LNCaP cells separated by a magnet. *Note*. From "Multifunctional plasmonic shell–magnetic core nanoparticles for targeted diagnostics, isolation, and photothermal destruction of tumor cells", by Z. Fan, M. Shelton, A.K. Singh, et al, 2012, *ACS Nano*, 6, p. 1065–73. Copyright 2012, *American Chemical Society*. Reprinted with permission.

transverse flow that facilitates effective contact between antigens on the cells and antibodies on the channel surface (Fig. 6B and C) [21].

For CTC isolation, the GASI chip was tested using blood samples from patients with several kinds of metastatic cancers [21]. Blood samples (1 mL) were collected from patients with breast, lung, or gastric cancers. After the samples passed through the GASI chip, the collected cells were fixed on a glass slide and stained with DAPI for DNA content, phycoerythrin-conjugated cytokeratins for CTCs, and FITC-conjugated CD45 for leukocytes. After fluorescence imaging of the glass slides, the captured images were carefully examined according to predefined criteria (DAPI positive, cytokeratin positive, CD45 negative), as shown in Fig. 7. Because the negative enrichment

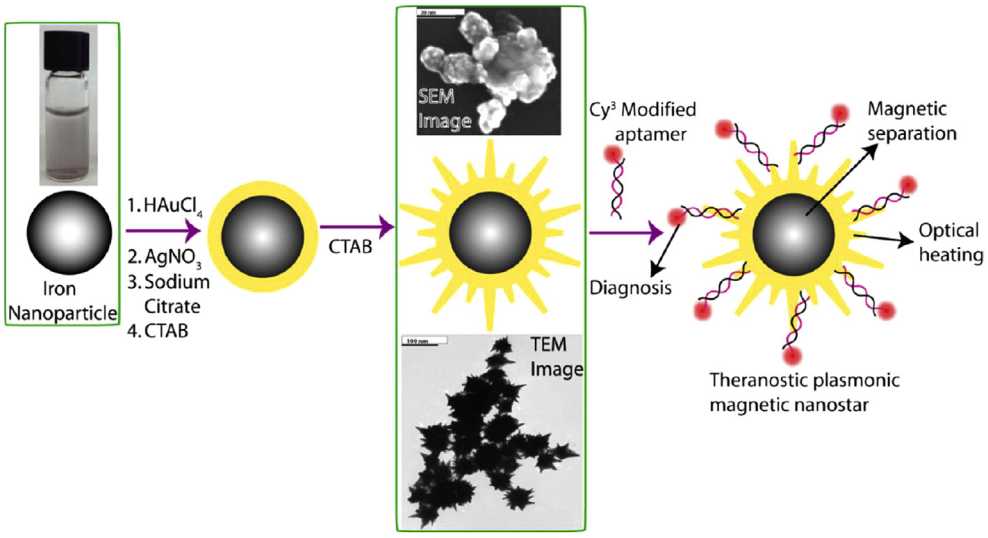

Fig. 4 – Schematic representation showing the synthesis of S6 aptamer-conjugate multifunctional theranostic magnetic core-gold shell star shaped nanoparticles. *Note.* From "Theranostic magnetic core–plasmonic shell star shape nanoparticle for the isolation of the targeted rare tumor cells from whole blood, fluorescence imaging, and photothermal destruction of cancer", by Z. Fan, D. Sanapati, A.K. Singh, et al, 2012, *Mol Pharm*, 10, p. 857–66. Copyright 2012, *American Chemical Society*. Reprinted with permission.

system does not use any characteristics of the target cells such as size or molecular surface markers, but only specifically removes nontarget cells [21], it can separate CTCs with a variety of features (Fig. 7).

4. Theranostic nanomedicine for cancer therapy

Cancer nanotechnology therapeutics is different from simple carriers of drugs or biomolecules (i.e., proteins, siRNA) [22]. Theranostic nanomedicine offers an opportunity to overcome limitations stated earlier. There are several potential advantages of conjugate drugs with nanoparticles, including targeted delivery of drugs to tumor sites [23], controlled release of specific drugs at different locations [24], and with increased half-life of drugs at disease sites by changing their pharmacokinetic profile [25]. One way to overcome these limitations is to engineer nanomaterials for active binding to specific cells after extravasation. This selective binding can be achieved by conjugating biomolecules (antibodies, aptamers, peptide, etc.) with nanomaterials through chemical bonding [26]. These functionalized nanomaterials will recognize and bind target cells, and the bound

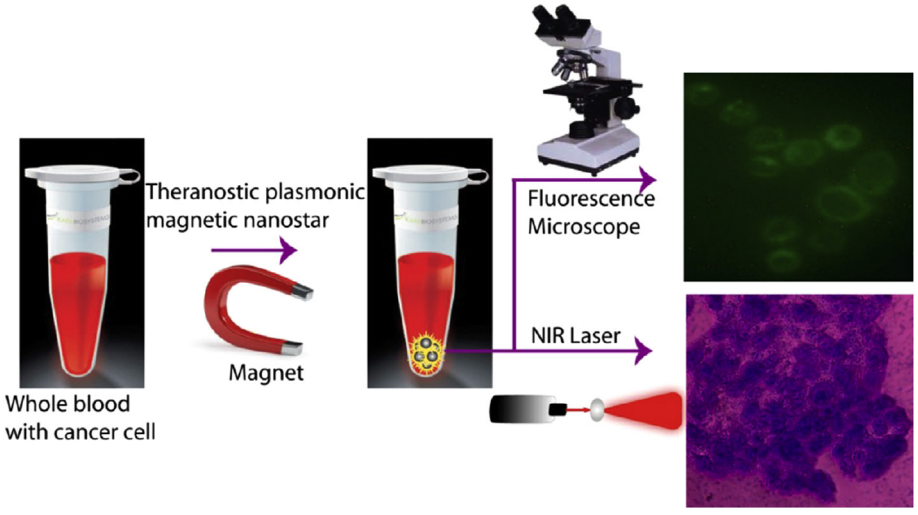

Fig. 5 – Schematic representation showing the separation of specific cancer cells using S6 aptamer-conjugated plasmonic/magnetic nanoparticles. *Note.* From "Theranostic magnetic core–plasmonic shell star shape nanoparticle for the isolation of the targeted rare tumor cells from whole blood, fluorescence imaging, and photothermal destruction of cancer", by Z. Fan, D. Sanapati, A.K. Singh, et al, 2012, *Mol Pharm*, 10, p. 857–66. Copyright 2012, *American Chemical Society*. Reprinted with permission.

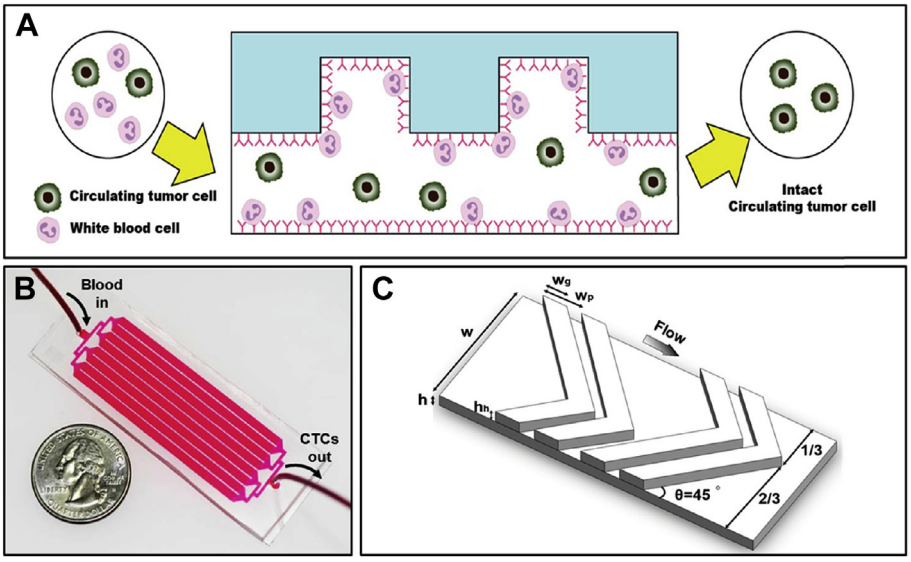

Fig. 6 – (A) Pictorial presentation of negative enrichment (side view). When the blood sample enters the inlet, the nontarget cells (i.e., leukocytes) are specifically captured on the CD45 antibody-coated channels, whereas the target cells (i.e., CTCs) are eluted through the outlet. The ridges on the top of the main straight channel create a helical flow that creates considerable interaction between the cells and the antibody-coated channel surface. (B) A photograph of the fabricated GASI chip. The GASI chip consists of an inlet, eight channels, and an outlet. Each channel is 2.1 mm in width and 50 mm in length. To prevent breakdown of the PDMS channel due to their flexibility, a wall 400 μm in width bears the pressure. (C) The herringbone structure and key parameters used in this study. *Note.* From "Negative enrichment of circulating tumor cells using a geometrically activated surface interaction chip", by K.A. Hyun, T.Y. Lee, and H.I. Jung. 2013, *Anal Chem*, 8, p. 4439–45. Copyright 2013, *American Chemical Society*. Reprinted with permission.

carriers are internalized inside the cell prior to when the drug is released. Another way is to skip chemotherapy and apply other treatment methods, such as photothermal therapy (PTT) and photodynamic therapy (PDT). PTT (use of heat to kill cancer cells) can be enhanced magnificently by applying desired nanomaterials with near infrared light [27], magnetic fields [28], and radio frequency [29]. PDT is also a clinical treatment where tumor cells are killed by the

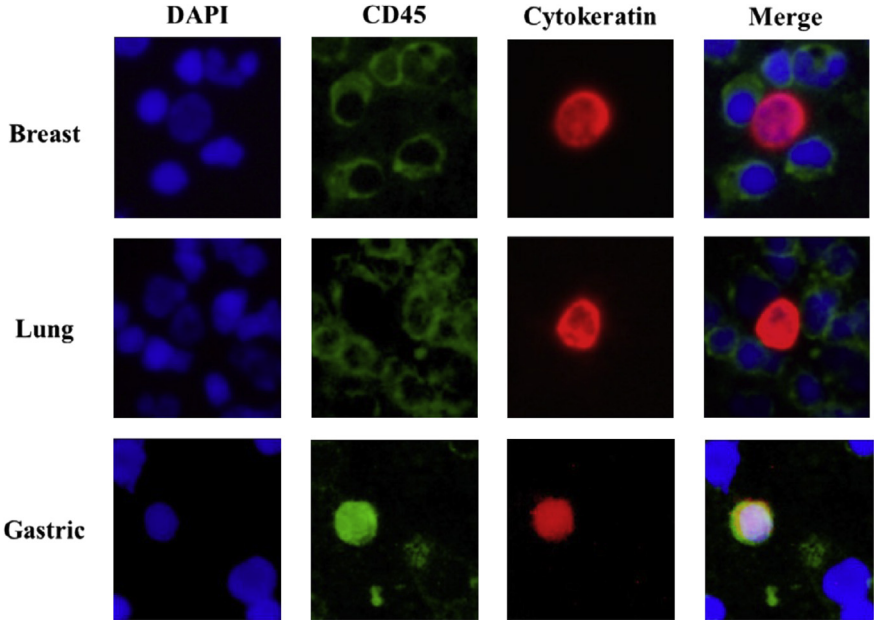

Fig. 7 – Fluorescence images of cells isolated using GASI chip from patients with metastatic cancers. For gastric cancer, all cytokeratin-positive cells appear dual-positive with CD45. *Note.* From "Dextran-coated iron oxide nanoparticles: a versatile platform for targeted molecular imaging, molecular diagnostics, and therapy", by C. Tassa, S.Y. Shaw, and R. Weissleder. 2011, *Acc Chem Res*, 44, p. 842–52. Copyright 2013, *American Chemical Society*. Reprinted with permission.

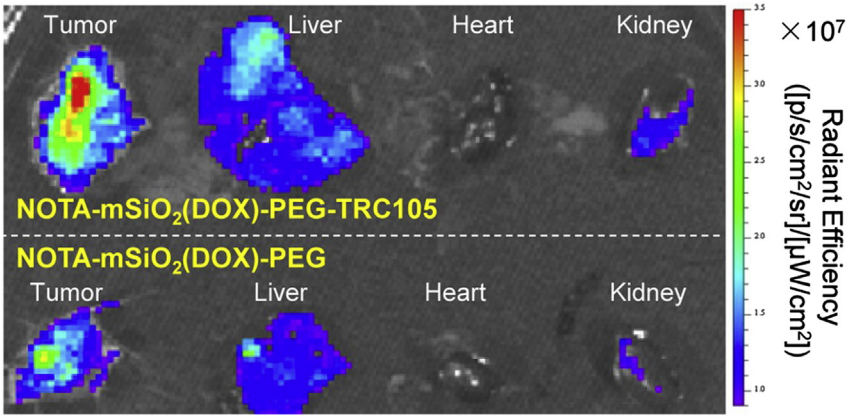

Fig. 8 – An *ex vivo* optical image of major organs at 0.5 hours after intravenous injection of NOTA-mSiO$_2$(DOX)-PEG-TRC105 in 4T1 tumor-bearing mice, which clearly showed stronger tumor DOX signal in the former. *Note.* From "*In vivo* tumor targeting and image-guided drug delivery with antibody-conjugated, radiolabeled mesoporous silica nanoparticles", by F. Chen, H. Hong, Y. Zhang, et al, 2013, *ACS Nano*, 7, p. 9027–39. Copyright 2013, *American Chemical Society*. Reprinted with permission.

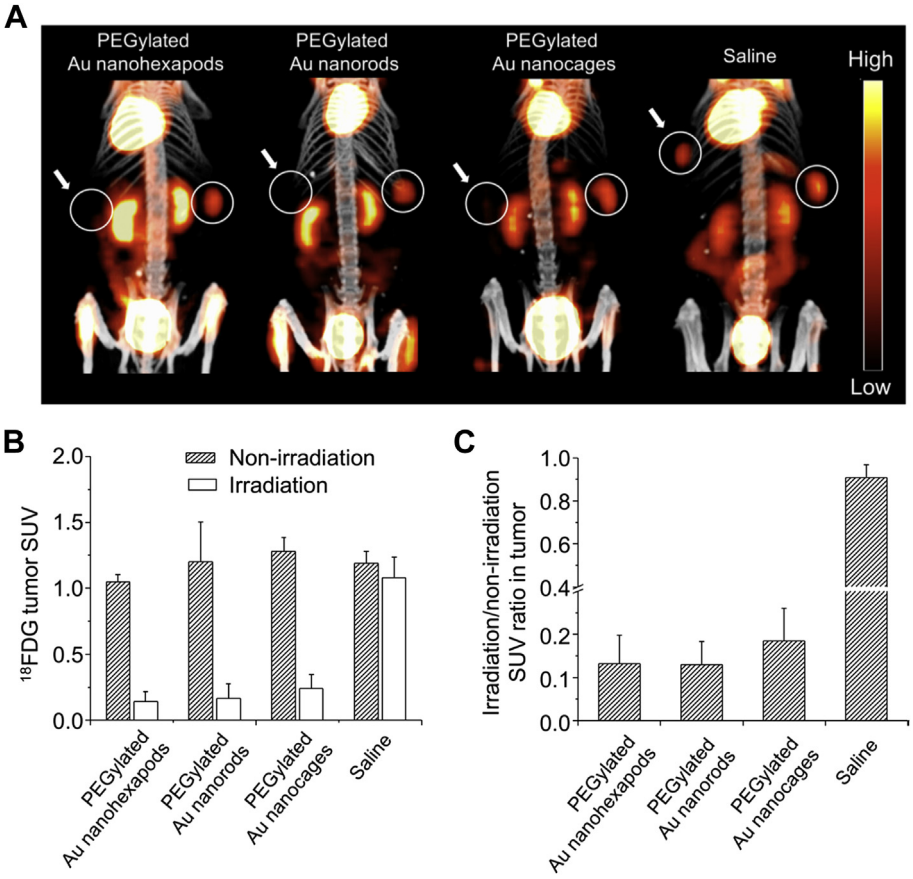

Fig. 9 – (A) ^{18}F- fluorodeoxyglucose (FDG) positron emission tomography–computed tomography coregistered images of mice intravenously administrated with aqueous suspensions of polyethylene glycol (PEG)ylated nanohexapods, nanorods, nanocages, or saline. Tumors were treated either with (solid circle + left arrow) or without (solid circle) laser irradiation. (B) ^{18}F-FDG standardized uptake values (SUVs) in laser-treated tumor and nontreated tumor. (C) Ratios of laser-treated tumor to non-treated tumor ^{18}F-FDG SUVs. Error bars are standard errors with $n = 3$. Note. From "Comparison study of gold nanohexapods, nanorods, and nanocages for photothermal cancer treatment", by Y. Wang, K.C.L. Black, H. Luehmann, et al, 2013, *ACS Nano*, 7, p. 2068–77. Copyright 2013, *American Chemical Society*. Reprinted with permission.

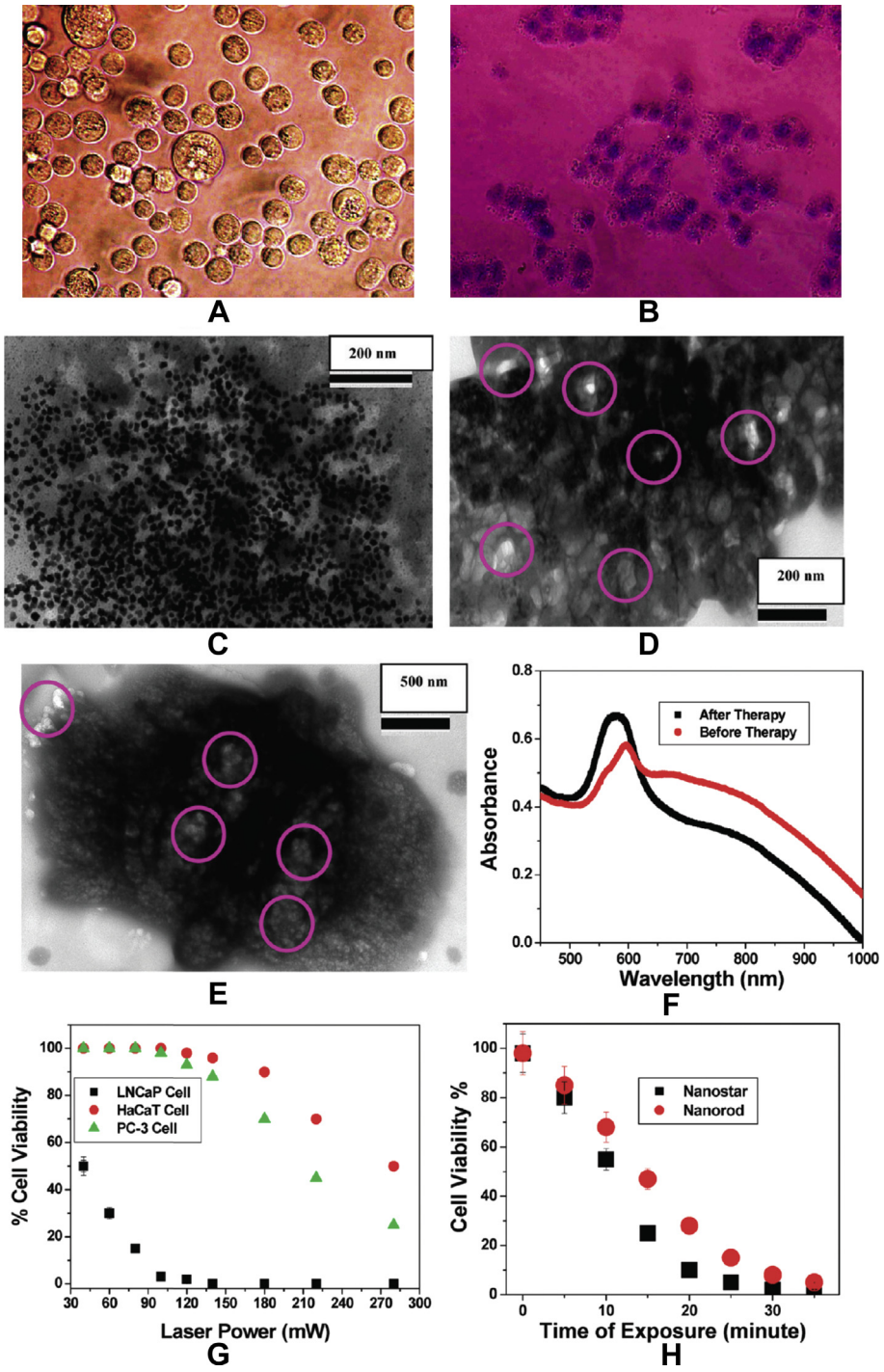

Fig. 10 – Bright-field inverted microscope images of multifunctional popcorn-shaped gold nanoparticle-conjugated LNCaP prostate cancer cells. (A) prior to therapy and (B) after therapy for 30 minutes and stained with trypan blue. (C) Transmission electron microscopy (TEM) images showing the deformation of cells after exposed to popcorn-shaped gold nanoparticle-conjugated LNCaP cells and 100 mW, 785 nm NIR continuous-wave radiation for 10 minutes. (D) TEM image showing structure deformation and irreparable damage of cancer cell surfaces after 20 minutes of radiation; purple circles show bubble formation. (E) TEM image demonstrating irreparable damage of cancer cell surfaces when multifunctional popcorn-shaped gold nanoparticle-conjugated LNCaP were exposed to 100 mW, 785 nm near infrared (NIR) continuous-wave radiation for 30 minutes; purple circles show bubble formation. (F) Absorption profile demonstrating nanoparticle structural changes after nanotherapy process. (G) Cell viability by 3-(4,5-dimethylthiazol-2-yl)-2,5-diphenyltetrazolium bromide test after popcorn-shaped gold nanoparticle-conjugated LNCaP cells, PC-3 cells, and HaCaT cells were exposed to 785 nm NIR continuous-wave radiation at different doses. (H) Comparison of photothermal therapy responses between well-characterized gold nanorods and popcorn-shaped gold nanoparticles when multifunctional nanoparticle-conjugated LNCaP

combination of light and a photosensitizer. These components, in addition to molecular oxygen in the tissue, generate cytotoxic singlet oxygen under proper dosage. Functionalized nanoparticle is complementary and supplementary to PDT [30] and helps to reach deeper tissue that PDT is not able to reach.

5. Selective drug delivery and encapsulation for chemotherapy

The application of gold nanoparticles as drug delivery vehicles has been reported by several groups. More complex delivery-related capabilities derived from functionalized nanoparticles, i.e., the administration of immunotherapy with a targeting ligand [31], administration of a prodrug with its activator enzyme [32]. The physiological microenvironment [33], ultrasound [34], light [35], or radio frequency electromagnetic fields [36] could all be used to release drug selectively.

In vivo enhanced anticancer drug delivery remains a major challenge in cancer nanotechnology. Recently, the development of functionalized uniform mesoporous silica ($mSiO_2$) nanoparticles for drug delivery in 4T1 murine breast tumor-bearing mice has been reported by Chen et al [37]. Besides gold nanoparticles, $mSiO_2$ nanoparticle is an alternative nanoplatform for selective drug delivery. In that report, uniform $mSiO_2$ nanoparticles were functionalized with SH-PEG, TRC105 antibody (specific to CD105/endoglin), Cu labeling and doxorubicin (DOX) [37]. After intravenous injection of functionalized $mSiO_2$ loaded with DOX into 4T1 tumor-bearing mice, an IVIS spectrum *in vivo* imaging system (excitation: 465 nm; emission: 580 nm) was applied to check nanoparticle distribution in the major organs (Fig. 8). The imaging showed the feasibility to deliver a certain amount of drugs (like DOX) selectively to the tumor site *in vivo* through functionalized $mSiO_2$ nanoparticles [37].

6. Selective near infrared light-induced PTT

Gold nanoparticles absorb light and convert photon energy efficiently to heat, which makes them superior agents for PTT. Gold nanoparticle-induced PTT has been popularly reported and tested in recent years [38–43]. It was first reported in 2003 for PTT of lymphocytes *in vitro* by gold nanoparticles with a nanosecond neodymium-doped yttrium aluminum garnet-pulsed laser at 532 nm, which caused cell destruction [38]. When irradiated with the specific laser light, functionalized gold nanomaterials will generate heat to kill cancer cells [39]. It was found that localized temperature increased to 70–80 °C through light absorption of gold nanoparticles [40] and around 150 antibodies were conjugated to PEG coated nanoshells [41]. Most of these studies were targeted on either epidermal growth factor receptor or HER2, because of the matched monoclonal antibodies already approved by the US Food and Drug Administration (FDA) for cancer therapy.

Because the absorbance wavelength of small gold nanospheres is not ideal for *in vivo* application, nanomaterials such as gold nanorods, nanocages, and nanohexapods, which have strong absorbance in the near infrared (NIR) range, have been tested for *in vivo* photothermal therapy. The development of gold nanohexapods as *in vivo* photothermal agents has been reported recently [42]. The localized surface plasmon resonance peaks of gold nanohexapods can be tuned by changing the length of the arms to NIR range for better penetration of the laser into body tissues. In addition, photothermal effect of gold nanohexapods was compared to those of gold nanorods and nanocages. ^{18}F-fluorodeoxyglucose (FDG) positron emission tomography–computed tomography was applied to observe tumor metabolism after targeted photothermal treatment with nanomaterials by Wang et al [42]. After intravenous injections of these three types of PEG coated gold nanomaterials or saline, ^{18}F-FDG positron emission tomography–computed tomography was performed prior to and after laser treatment. The ^{18}F-FDG uptake was distinctly reduced within laser treated tumors compared to non-irradiated tumors (Fig. 9A). After the laser treatment, substantial decrease of tumor standardized uptake values were noticed, whereas the untreated tumors showed constant metabolism (Fig. 9B). Nearly 90% reduction of tumor metabolism in mice treated with nanohexapods or nanorods and 80% decrease in mice treated with nanocages were observed (Fig. 9C). These results demonstrate that all these PEG coated gold nanomaterials could work as effective photothermal agents for treatment of cancer.

The nanotechnology-driven, multifunctionalized gold nanopopcorns can also be applied for targeted PTT treatment. NIR radiation was applied for PTT. In this report [43], a continuous-wavelength portable OEM laser operating at 785 nm was used as the excitation light source for 30 minutes. After that, a 3-(4,5-dimethylthiazol-2-yl)-2,5-diphenyltetrazolium bromide (MTT) cell viability test was performed to find the amount of live cells during the nanotherapy process. During PTT, light absorbed by the gold nanoparticles is transferred to the antibody, aptamer, and cell environment by rapid electron-phonon relaxation in the nanoparticles, followed by phonon-phonon relaxation [43–46]. This irradiation wavelength matches the plasmon bands of the LNCaP cancer cell-conjugated popcorn-shaped gold nanoparticles. As shown in Fig. 10, exposure to the 785 nm light at 100 mW (12.5 W/cm^2) caused photothermal destruction of all the prostate cancer cells. Transmission electron microscopy images (Fig. 10D and E) of the irradiated cells clearly show areas of massive, irreparable cell membrane disruption. After therapy, cell viability was tested by MTT as well as bright-field inverted microscopy. Trypan blue was applied to determine the extent of cell death. Fig. 10A shows that cells are 100% alive without therapy, but

cells were exposed to 100 mW, 785 nm NIR continuous-wave radiation for different times. *Note*. From "Gold nano-popcorn-based targeted diagnosis, nanotherapy treatment, and *in situ* monitoring of photothermal therapy response of prostate cancer cells using surface-enhanced Raman spectroscopy", by W. Lu, A.K. Singh, S.A. Khan, et al, 2010, *J Am Chem Soc*, 13, p. 18103–14. Copyright 2010, American Chemical Society. Reprinted with permission.

Fig. 10B shows that most of the cancer cells are dead after 30 minutes of the nanotherapy process. The bright-field inverted microscope image shows that the cancer cells are deformed due to the nanotherapy process. This cell death following nanoparticles exposure to NIR radiation could be due to numerous factors including nanoparticle explosion, shock waves, bubble formation, and thermal disintegration. As shown in Fig. 10D and E, bubbles are formed (indicated by purple circles) when multifunctional popcorn-shaped gold nanoparticle-conjugated LNCaP cells were exposed to 100 mW, 785 nm NIR continuous wave radiation. As measured, the temperature increases to 48 °C during the nanotherapy process. As shown in Fig. 10H, the time-interval MTT test indicates that, within 30 minutes, most of the cancer cells died. The same tests for the prostate specific membrane antigen-negative prostate cancerous (PC-3) and noncancerous (HaCaT) cells (Fig. 10G) were also performed. The cancer cells required less than half the laser energy (8 W/cm^2) for photothermal lysis in comparison to the normal cells (20 W/cm^2). To understand how good the PTT is with the popcorn-shaped gold nanoparticles, the same photothermal experiment with multifunctional gold nanorods ($\alpha = 2.3$) was performed using 100 mW, 785 nm NIR continuous-wave radiation. Fig. 10H shows that photothermal response for nanopopcorn-based gold nanoparticles is comparable or slightly better than that of the well-studied gold nanorods.

In addition to early detection and isolation of cancer cells, multifunctional plasmonic shell-magnetic core nanoparticles can also work as photothermal agent to kill cancer cells, as reported recently [15]. Due to good biocompatibility, nontoxic, and with the ability to generate high temperatures at a desired site, the greatest promise of plasmonic gold nanotechnology medicine will be its use for early detection and therapeutics of cancers [9,15,16,18,24,25,27,48,49,57–59]. Similarly, magnetic nanoparticles can also mediate localized hyperthermal effects in the presence of a strong magnetic field [10–20]. In the photothermal destruction experiment, 670 nm red light at 2–3 W/cm^2 was used for 10 minutes' irradiation. Because biological systems mostly lack chromophores that absorb the NIR light of 650–900 nm [48,49,51,58–71], 670 nm is particularly useful in therapy for the induction of hyperthermia. When S6-modified magnetic/plasmonic nanoparticles bound to SK-BR-3 cells are excited with 670 nm light, due to the strong absorption at this wavelength, photoexcitation of the electron gas resulted in rapid nonequilibrium heating [15]. As shown in Fig. 11A, most of the cancer cells were dead after 7 minutes of the nanotherapy process. Bright-field inverted

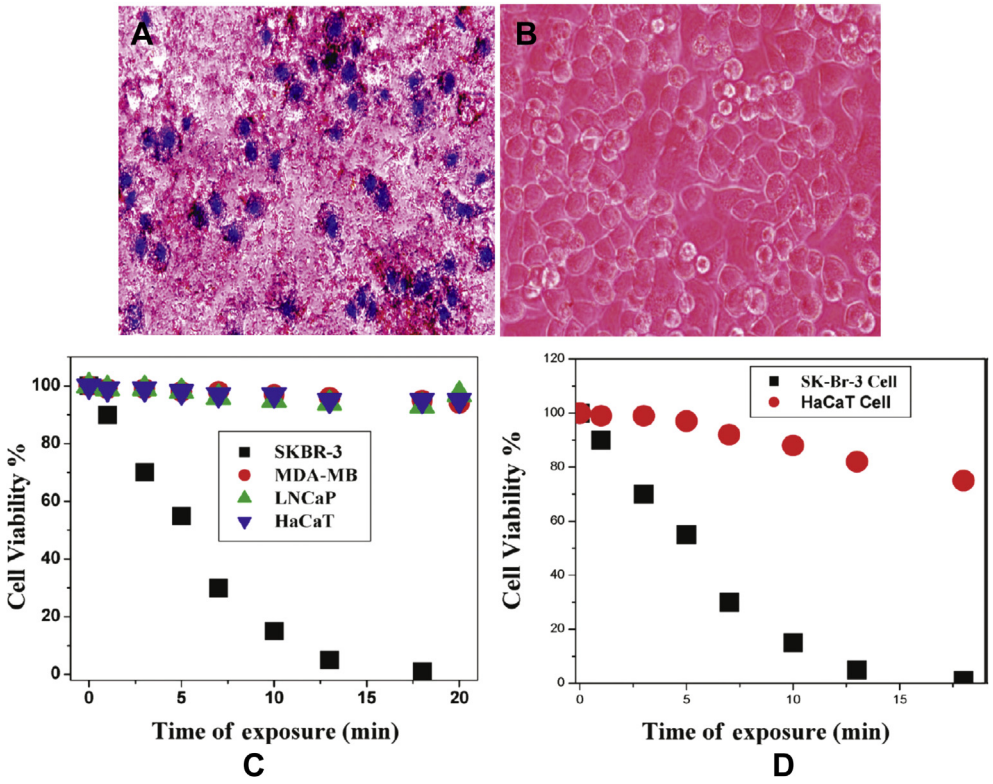

Fig. 11 – (A) Bright-field inverted microscopic images of aptamer-conjugated magnetic/plasmonic nanoparticles attached to SK-BR-3 breast cancer cells after irradiation with 670 nm light at 2.5 W/cm^2 for 7 minutes followed by staining with trypan blue. (B) The same experiment as in (A) for SK-BR-3 cells. (C) Cell viability when S-6 aptamer-conjugated magnetic/plasmonic nanoparticles attached to SK-BR-3, MDA-MB, and HaCaT cells were treated using 670 nm light at 2.5 W/cm^2 for 20 minutes. (D) Cell viability when S-6 aptamer-conjugated magnetic/plasmonic nanoparticles attached to SK-BR-3 and HaCaT cell mixtures (1:0.01) were treated 670 nm light at 2.5 W/cm^2 for 20 minutes. *Note.* From "Multifunctional plasmonic shell–magnetic core nanoparticles for targeted diagnostics, isolation, and photothermal destruction of tumor cells", by Z. Fan, M. Shelton, A.K. Singh, et al, 2012, *ACS Nano*, 6, p. 1065–73. Copyright 2012, *American Chemical Society*. Reprinted with permission.

microscope images show that cancer cells were deformed during the nanotherapy process. To understand how much the temperature increases was during photothermal destruction, thermal imaging was taken at 1-minute intervals during the therapy process using a Mikro-Shot camera. The temperature increased to about 55 °C when exposing to magnetic/plasmonic nanoparticle-bound cancer cells to a 670 nm laser at 2.5 W/cm^2. By contrast, under the same conditions, the temperature increased to only 35 °C for MDA-MB and LNCaP cancer cells without any nanoparticles.

As shown in Fig. 11C, the time interval cell viability test indicated that, within 10 minutes, most of the SK-BR-3 cancer cells were killed. By contrast, cell viability was more than 93% in the MDA-MB and LNCaP cells and 96% for the HaCaT cells. This is because the cancer cells are conjugated with the magnetic/plasmonic nanoparticles with strong absorption at the excitation wavelength of 670 nm [15]. As shown in Fig. 11D, normal cells started to die after 6 minutes of therapy. At 13 minutes, about 100% of cancer cells were dead, only 12% of normal cells were dead. In this way, this photothermal destruction was highly selective.

7. Selective combined therapy

PDT is one of the most important therapeutic options for cancer and other diseases [47,49,60–62,71]. Despite its advantage over traditional treatments, PDT has not been accepted for general treatment in clinic [47,49,60–62,71]. There are several technical difficulties for the application of PDT. First, the photosensitizers for PDT approved by the FDA absorb light with wavelength below 700 nm, which does not show good light penetration in the body [47,49,60–62,71]. Second, most existing photosensitizers aggregate easily under physiological conditions. Third, the photosensitizers have low selectivity to disease tissues [47,49,60–62,71].

Nanoparticles, by contrast, offer possible solutions for these problems. Photosensitizer-conjugated nanoparticles can be coated with PEG and modified with monoclonal antibodies to selectively target the disease tissues [47,49,60–62,71]. Through two-photon excitation of the dyes encapsulated by nanoparticles, it is possible to activate photosensitizers with low energy light that can deeply penetrate tissues. The process for delivery of photosensitizers is divided into passive and active, based on the presence or absence of the targeting molecules on the surface [23]. In this way, the methods to deliver photosensitizers specifically to disease tissues are named active, whereas other methods which apply parenteral administration and passive targeting (liposomes, polymeric particles, and hydrophilic polymer-photosensitizer conjugates) are named passive [47,49,60–62,71]. Biodegradable polymeric nanoparticles, which received tremendous attention as a possible method of delivering agents, are the main passive carriers. The main advantages are high drug loading

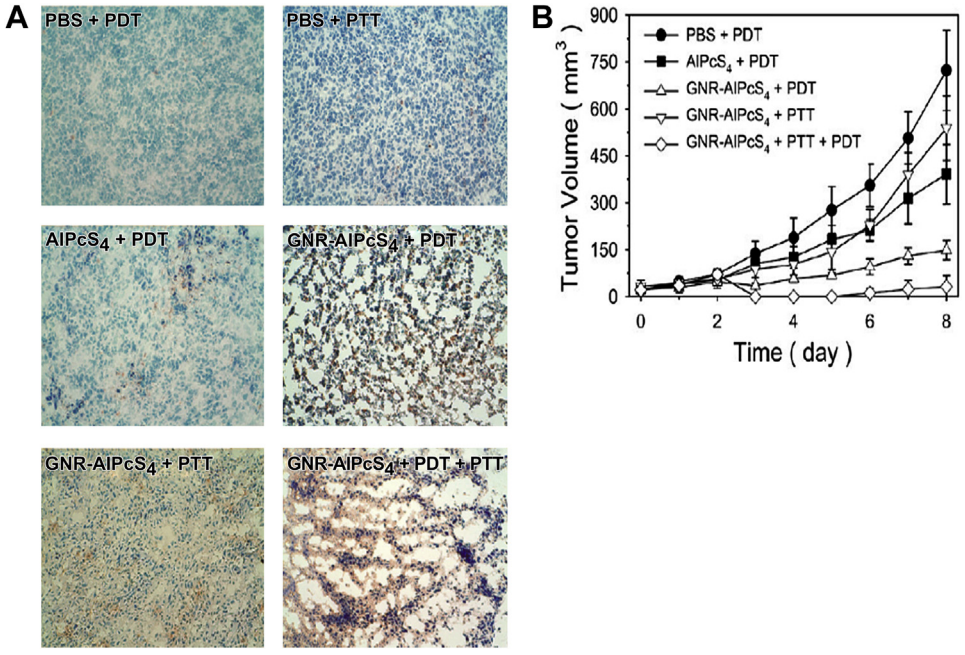

Fig. 12 – *In vivo* photodynamic therapy (PDT) and photothermal therapy (PTT). (A) TUNEL staining of the tissue sections (magnification ×20). Normal or apoptotic cell nuclei are shown in green and brown, respectively. Empty areas in the tissue sections (GNR–AlPcS$_4$) complex + PDT and GNR–AlPcS$_4$ complex + PTT + PDT) are due to washout of the destroyed tumor cells during the staining procedure. (B) Tumor size after each therapy session. Points, mean; bars, standard deviation; phosphate buffered saline + PDT (n = 7); free AlPcS$_4$ + PDT (n = 7); GNR–AlPcS$_4$ complex + PDT (n = 7); GNR–AlPcS$_4$ complex + PTT (n = 5); GNR–AlPcS$_4$ complex + PTT + PDT (n = 7); n = number of tumors involved. *Note.* From "Gold nanorod–photosensitizer complex for near-infrared fluorescence imaging and photodynamic/photothermal therapy *in vivo*", by B. Jang, J.Y. Park, C.H. Tung, et al, 2011, *ACS Nano*, 5, p. 1086–94. Copyright 2011 American Chemical Society. Reprinted with permission.

ability, selective drug release, and a variety of available materials and manufacturing processes [45]. Photosensitizer nanoparticles as one kind of active carriers have been the focus of attention. Quantum dots are nanosized imaging probes with high quantum yields, high photostability and fluorescent emission ability which can be tuned by size. They can be synthesized in aqueous solutions for a specific target to pathological areas. Energy can be transferred to surrounding O_2 by

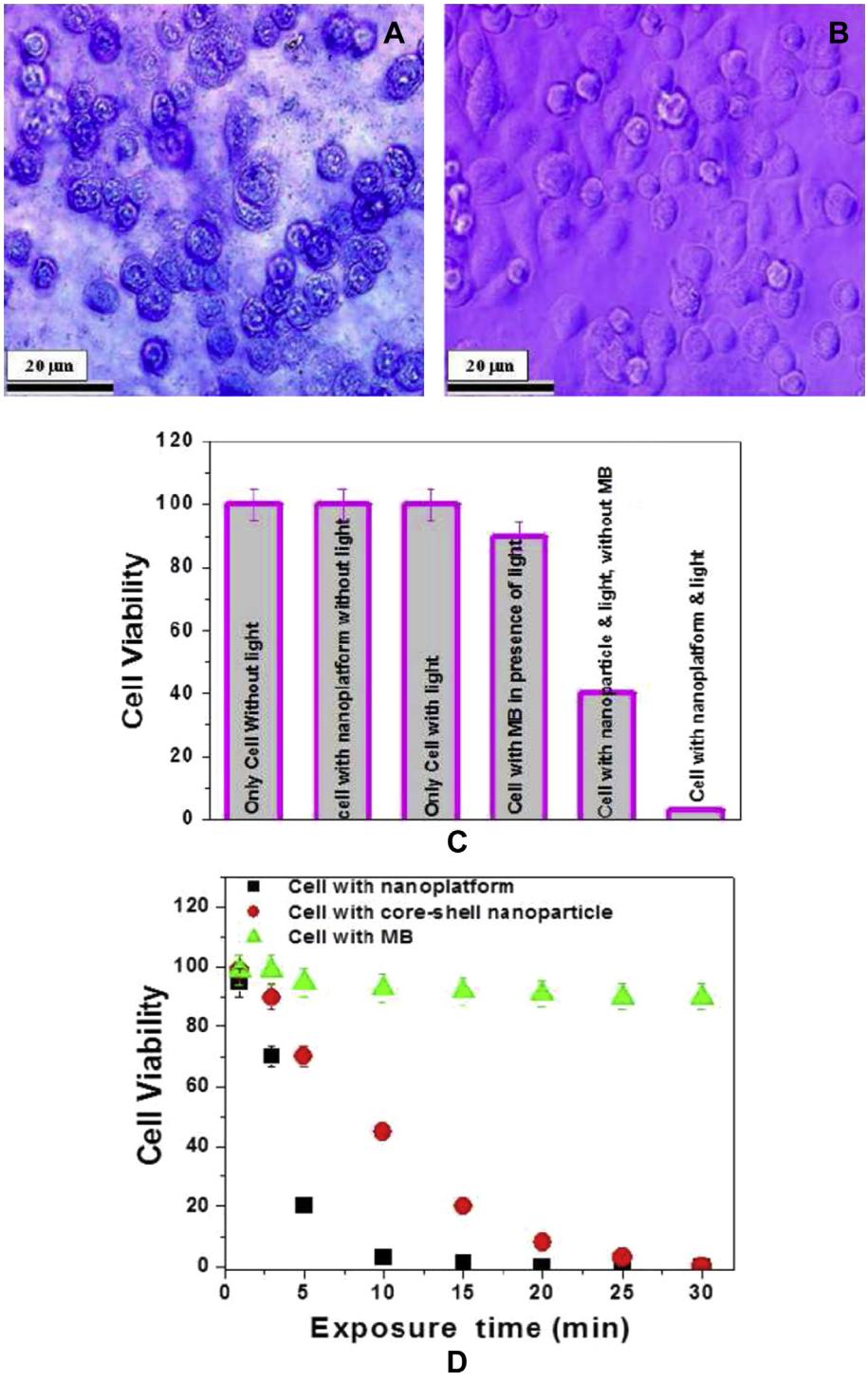

Fig. 13 – (A) Bright-field inverted microscopic images of methylene blue (MB)-bound nanoplatforms attached LNCaP cell separated by a magnet followed by irradiation with 785 nm near IR light at 1 W/cm^2 for 7 minutes and stained with trypan blue. (B) Bright-field inverted microscopic images of LNCaP cells in the absence of nanoplatforms or MB and irradiated with 785 nm light at 1 W/cm^2 for 20 minutes followed by staining with trypan blue. (C) Cell viability in MB-bound nanoplatforms attached LNCaP cells in the absence or presence of laser light. No cytotoxicity in the absence of NIR light. It also shows dramatic synergistic action in case of combined therapy. (D) Time-dependent cell viability after irradiation with 785 nm near IR light at 1–2 W/cm^2 for 35 minutes, in case of photodynamic, photothermal, and combination therapy.

quantum dots, leading to toxicity to cells. Their potential application as photosensitizers has been explored in recent reports [46].

A gold nanorod-photosensitizer conjugate was developed for NIR photodynamic and photothermal combined therapy *in vivo* [47]. When the gold nanorod (GNR) and the photosensitizer conjugate are targeted to the surface of the tumor tissue, the photosensitizers will be released from the GNR to tissue surface and will generate singlet oxygen. The tumor tissues can be selectively damaged by NIR laser irradiation during targeted PDT while minimizing phototoxic tissue destruction of surrounding healthy tissues. Therapeutic efficacy of gold nanorod and photosensitizer conjugates can be enhanced by extra photothermal therapy from gold nanorod. A xenografted mouse tumor modal was applied to test the combined therapy from a GNR-photosensitizer complex. After intravenous injection with phosphate buffered saline, free photosensitizer (tetrasulfonated aluminum phthalocyanine, $AlPcS_4$), and GNR–$AlPcS_4$ complex, *in vivo* therapeutic efficacy was investigated. Tumor damage was not observed for phosphate buffered saline-injected mice after PDT and PTT (Fig. 12A). $AlPcS_4$-treated mice showed some tissue damage after PDT. Mice injected with GNR–$AlPcS_4$ showed severe tissue loss across a large tumor area. The efficacy of GNR–$AlPcS_4$ treatment was also evaluated by measuring tumor growth rates (Fig. 12B). Tumor growth decreased 79% with PDT alone and 95% with combined PTT and PDT.

In addition, the theranostic plasmonic shell-magnetic core star shaped nanomaterials was not only applied for targeted isolation and detection of rare tumor cells from whole blood, but also used as agents for combined synergistic photothermal and photodynamic treatment of cancer. Several groups have shown that magnetic core-plasmonic shell nanoparticles can be used for PDT of cancer cell [48]. Methylene blue is a well-known PDT agent [49]. The methylene-blue bound magnetic core-plasmonic shell nanoplatform based combined photodynamic and photothermal synergistic targeted therapy of cancer was researched. The magnetic core can be used for rare tumor cell isolation and enrichment. Methylene blue-modified A9 aptamers are attached to nanoplatform through –SH linkage for: (1) specific LNCaP prostate cancer cell recognition which overexpress prostate specific membrane antigen, via the A9 aptamers [48]; (2) fluorescence imaging using methylene blue as the fluorescence probe; and (3) targeted PDT using methylene blue. By contrast, functionalized nanoparticles have been used as a photothermal agent. The existing results show that the cancer cells can be selectively separated, imaged, and destroyed significantly by illumination with 785 nm NIR continuum wave light for a few minutes. Due to the synergistic effect, the therapeutic efficacy of nanoplatform was enhanced significantly compared to PDT or PTT alone. Because the clinically ideal phototherapeutic biological window for cancer is between 700 nm and 1100 nm [50], the magnetic core-plasmonic shell nanoplatform has strong absorption at 785 nm, the 785 nm NIR laser was applied for combined synergistic therapy for cancer tumor. Bright-field inverted microscope images (Fig. 13A) show that LNCaP cancer cells are deformed during the combined therapy process. The cell death following nanoplatform exposure to NIR radiation could be due to numerous factors including reactive oxygen species-induced cell death, nanoparticle explosion, shock waves, bubble formation, and thermal disintegration. Fig. 13B shows that the bright field inverted microscope images of LNCaP cells in the absence of nanoplatform and methylene blue, after 20 minutes of exposure by 785 nm laser. Bright field image and MTT test clearly showed no cell death in the absence of nanoplatform. The nanoplatform-based combined therapeutic killing is highly selective for the cells attached with nanoplatform, and the combined therapy can only be activated in the presence of NIR laser. Fig. 13C and D show that when the two treatments were combined under a single irradiation, the cell viability was remarkably reduced, which is much lower than that treated individually.

8. Cancer nanotechnology: future and challenges

Nanomaterials are potential tools of tremendous benefits that are now starting to be applied in the clinic. Targeting ligands, imaging agents, and drug delivery can all be integrated into one functionalized nanoparticle for targeted imaging and therapy. Thus multifunctionality is a unique advantage of nanomaterials over traditional treatments. Developing nanoparticle diagnosis and therapy in the right directions will greatly improve the outcome of cancer patients. The future of cancer nanotechnology lies on a multifunctional nanoplatform that combines both therapeutic components and multimodality imaging. The ultimate goal is that multifunctional nanomedicine works as efficient, targeted *in vivo* drug delivery without systemic toxicity, and the dose delivered as well as the therapeutic efficacy can be accurately measured noninvasively with time. Much remains to be done prior to when this can be transferred into the clinic and many factors need to be optimized simultaneously for the best clinical outcome.

Conflicts of interest

All contributing authors declare no conflicts of interest.

Acknowledgments

We thank Dr Jiekun Xuan for critical review of this manuscript. We are grateful for NSF-PREM funding (No. DMR-1205194) for nanomaterial and bioimaging.

REFERENCES

[1] Siegel R, Naishadham D, Jemal A. Cancer statistics, 2013. CA Cancer J Clin 2013;63:11–30.
[2] WHO Media Centre. Fact Sheet No. 297. Cancer. Available at: www.who.int/mediacentre/factsheets/fs297/en/ Accessed Oct. 2013.

[3] Ashworth TR. A case of cancer in which cells similar to those in the tumours were seen in the blood after death. Aus Med J 1869;14:146–7.
[4] Talasaz AH, Powell AA, Huber DE, et al. Isolating highly enriched populations of circulating epithelial cells and other rare cells from blood using a magnetic sweeper device. Proc Natl Acad Sci U S A 2009;106:3970–5.
[5] Bray F, Møller B. Predicting the future burden of cancer. Nat Rev Cancer 2006;6:63–74.
[6] Danila DC, Fleisher M, Scher HI. Circulating tumor cells as biomarkers in prostate cancer. Clin Cancer Res 2011;17:3903–12.
[7] Jain PK, El-Sayed IH, El-Sayed MA. Au nanoparticles target cancer. Nano Today 2007;2:18–29.
[8] Budd GT. Let me do more than count the ways: what circulating tumor cells can tell us about the biology of cancer. Mol Pharm 2009;6:1307–10.
[9] Bardhan R, Lal S, Joshi A, et al. Theranostic nanoshells: from probe design to imaging and treatment of cancer. Acc Chem Res 2011;44:936–46.
[10] Eck W, Craig G, Sigdel A, et al. PEGylated gold nanoparticles conjugated to monoclonal F19 antibodies as targeted labeling agents for human pancreatic carcinoma tissue. ACS Nano 2008;2:2263–72.
[11] El-Sayed MA. Some interesting properties of metals confined in time and nanometer space of different shapes. Acc Chem Res 2001;34:257–64.
[12] Gupta GP, Massagué J. Cancer metastasis: building a framework. Cell 2006;127:679–95.
[13] Adams AA, Okagbare PI, Feng J, et al. Highly efficient circulating tumor cell isolation from whole blood and label-free enumeration using polymer-based microfluidics with an integrated conductivity sensor. J Am Chem Soc 2008;130:8633–41.
[14] Nagrath S, Sequist LV, Maheswaran S, et al. Isolation of rare circulating tumour cells in cancer patients by microchip technology. Nature 2007;450:1235–9.
[15] Fan Z, Shelton M, Singh AK, et al. Multifunctional plasmonic shell–magnetic core nanoparticles for targeted diagnostics, isolation, and photothermal destruction of tumor cells. ACS Nano 2012;6:1065–73.
[16] Fan Z, Senapati D, Singh AK, et al. Theranostic magnetic core–plasmonic shell star shape nanoparticle for the isolation of targeted rare tumor cells from whole blood, fluorescence imaging, and photothermal destruction of cancer. Mol Pharm 2012;10:857–66.
[17] Peleg G, Lewis A, Linial M, et al. Nonlinear optical measurement of membrane potential around single molecules at selected cellular sites. Proc Natl Acad Sci U S A 1999;96:6700–4.
[18] Famulok M, Hartig JS, Mayer G. Functional aptamers and aptazymes in biotechnology, diagnostics, and therapy. Chem Rev 2007;107:3715–43.
[19] Laurent S, Forge D, Port M, et al. Magnetic iron oxide nanoparticles: synthesis, stabilization, vectorization, physicochemical characterizations, and biological applications. Chem Rev 2008;108:2064–110.
[20] Tassa C, Shaw SY, Weissleder R. Dextran-coated iron oxide nanoparticles: a versatile platform for targeted molecular imaging, molecular diagnostics, and therapy. Acc Chem Res 2011;44:842–52.
[21] Hyun KA, Lee TY, Jung HI. Negative enrichment of circulating tumor cells using a geometrically activated surface interaction chip. Anal Chem 2013;85:4439–45.
[22] Wang J, Tian S, Petros RA, et al. The complex role of multivalency in nanoparticles targeting the transferrin receptor for cancer therapies. J Am Chem Soc 2010;132:11306–13.
[23] Park JH, von Maltzahn G, Ong LL, et al. Cooperative nanoparticles for tumor detection and photothermally triggered drug delivery. Adv Mater 2010;22:880–5.
[24] von Maltzahn G, Centrone A, Park JH, et al. SERS-coded gold nanorods as a multifunctional platform for densely multiplexed near-infrared imaging and photothermal heating. Adv Mater 2009;21:3175–80.
[25] Gabizon A, Shmeeda H, Barenholz Y. Pharmacokinetics of pegylated liposomal Doxorubicin: review of animal and human studies. Clin Pharmacokinet 2003;42:419–36.
[26] Torchilin VP. Recent advances with liposomes as pharmaceutical carriers. Nat Rev Drug Discov 2005;4:145–60.
[27] Lal S, Clare SE, Halas NJ. Nanoshell-enabled photothermal cancer therapy: impending clinical impact. Acc Chem Res 2008;41:1842–51.
[28] Baker I, Zeng Q, Li W, et al. Heat deposition in iron oxide and iron nanoparticles for localized hyperthermia. J Appl Phys 2006;99. 08H106–08H106-3.
[29] Yang W, Ahmed M, Elian M, et al. Do liposomal apoptotic enhancers increase tumor coagulation and end-point survival in percutaneous radiofrequency ablation of tumors in a rat tumor model? Radiology 2010;257:685–96.
[30] Samia ACS, Chen X, Burda C. Semiconductor quantum dots for photodynamic therapy. J Am Chem Soc 2003;125:15736–7.
[31] Poon Z, Chen S, Engler AC, et al. Ligand-clustered "patchy" nanoparticles for modulated cellular uptake and *in vivo* tumor targeting. Angew Chem Int Ed Engl 2010;49:7266–70.
[32] Gupta PB, Onder TT, Jiang G, et al. Identification of selective inhibitors of cancer stem cells by high-throughput screening. Cell 2009;138:645–59.
[33] Timko BP, Dvir T, Kohane DS. Remotely triggerable drug delivery systems. Adv Mater 2010;22:4925–43.
[34] Burks SR, Ziadloo A, Hancock HA, et al. Investigation of cellular and molecular responses to pulsed focused ultrasound in a mouse model. PLoS ONE 2011;6:e24730.
[35] Wu G, Mikhailovsky A, Khant HA, et al. Remotely triggered liposome release by near-infrared light absorption via hollow gold nanoshells. J Am Chem Soc 2008;130:8175–7.
[36] Derfus AM, von Maltzahn G, Harris TJ, et al. Remotely triggered release from magnetic nanoparticles. Adv Mater 2007;19:3932–6.
[37] Chen F, Hong H, Zhang Y, et al. *In vivo* tumor targeting and image-guided drug delivery with antibody-conjugated, radiolabeled mesoporous silica nanoparticles. ACS Nano 2013;7:9027–39.
[38] Pitsillides CM, Joe EK, Wei X, et al. Selective cell targeting with light-absorbing microparticles and nanoparticles. Biophys J 2003;84:4023–32.
[39] Huang X, El-Sayed IH, Qian W, et al. Cancer cell imaging and photothermal therapy in the near-infrared region by using gold nanorods. J Am Chem Soc 2006;128:2115–20.
[40] Huang X, Jain PK, El-Sayed IH, et al. Determination of the minimum temperature required for selective photothermal destruction of cancer cells with the use of immunotargeted gold nanoparticles. Photochem Photobiol 2006;82:412–7.
[41] Lowery AR, Gobin AM, Day ES, et al. Immunonanoshells for targeted photothermal ablation of tumor cells. Int J Nanomedicine 2006;1:149–54.
[42] Wang Y, Black KCL, Luehmann H, et al. Comparison study of gold nanohexapods, nanorods, and nanocages for photothermal cancer treatment. ACS Nano 2013;7:2068–77.
[43] Lu W, Singh AK, Khan SA, et al. Gold nano-popcorn-based targeted diagnosis, nanotherapy treatment, and *in situ* monitoring of photothermal therapy response of prostate cancer cells using surface-enhanced Raman spectroscopy. J Am Chem Soc 2010;132:18103–14.

[44] Ferrari M. Cancer nanotechnology: opportunities and challenges. Nat Rev Cancer 2005;5:161–71.
[45] Konan YN, Gurny R, Allémann E. State of the art in the delivery of photosensitizers for photodynamic therapy. J Photochem Photobiol B 2002;66:89–106.
[46] Bakalova R, Ohba H, Zhelev Z, et al. Quantum dots as photosensitizers? Nat Biotechol 2004;22:1360–1.
[47] Jang B, Park JY, Tung CH, et al. Gold nanorod–photosensitizer complex for near-infrared fluorescence imaging and photodynamic/photothermal therapy *in vivo*. ACS Nano 2011;5:1086–94.
[48] Santra S, Kaittanis C, Santiesteban OJ, et al. Cell-specific, activatable, and theranostic prodrug for dual-targeted cancer imaging and therapy. J Am Chem Soc 2011;133:16680–8.
[49] Noimark S, Dunnill CW, Kay CWM, et al. Incorporation of methylene blue and nanogold into polyvinyl chloride catheters; a new approach for light-activated disinfection of surfaces. J Mater Chem 2012;22:15388–96.
[50] Zamboni WC, Torchilin V, Patri AK, et al. Best practices in cancer nanotechnology: perspective from NCI nanotechnology alliance. Clin Cancer Res 2012;18:3229–41.
[51] Mieszawska AJ, Mulder WJM, Fayad ZA, et al. Multifunctional gold nanoparticles for diagnosis and therapy of disease. Mol Pharm 2013;10:831–47.
[52] Ray PC. Size and shape dependent second order nonlinear optical properties of nanomaterials and their application in biological and chemical sensing. Chem Rev 2010;110:5332–65.
[53] Kaittanis C, Santra S, Perez JM. Role of nanoparticle valency in the nondestructive magnetic-relaxation-mediated detection and magnetic isolation of cells in complex media. J Am Chem Soc 2009;131:12780–91.
[54] Lee GY, Qian WP, Wang L, et al. Theranostic nanoparticles with controlled release of gemcitabine for targeted therapy and MRI of pancreatic cancer. ACS Nano 2013;7:2078–89.
[55] Wisner ER, Katzberg RW, Griffey SM, et al. Characterization of normal and cancerous lymph nodes on indirect computed tomography lymphographic studies after interstitial injection of iodinated nanoparticles. Acad Radiol 1996;3(Suppl. 2):S257–60.
[56] Davis ME, Zuckerman JE, Choi CHJ, et al. Evidence of RNAi in humans from systemically administered siRNA via targeted nanoparticles. Nature 2010;464:1067–70.
[57] Louie A. Multimodality imaging probes: design and challenges. Chem Rev 2010;110:3146–95.
[58] Mulvey JJ, Villa CH, McDevitt MR, et al. Self-assembly of carbon nanotubes and antibodies on tumours for targeted amplified delivery. Nat Nano 2013;8:763–71.
[59] Sardana G, Jung K, Stephan C, et al. Proteomic analysis of conditioned media from the PC3, LNCaP, and 22Rv1 prostate cancer cell lines: discovery and validation of candidate prostate cancer biomarkers. J Proteome Res 2008;7:3329–38.
[60] Usacheva MN, Teichert MC, Biel MA. The role of the methylene blue and toluidine blue monomers and dimers in the photoinactivation of bacteria. J Photochem Photobiol B 2003;71:87–98.
[61] Tang W, Xu H, Park EJ, et al. Encapsulation of methylene blue in polyacrylamide nanoparticle platforms protects its photodynamic effectiveness. Biochem Biophys Res Commun 2008;369:579–83.
[62] Lovell JF, Liu TW, Chen J, et al. Activatable photosensitizers for imaging and therapy. Chem Rev 2010;110:2839–57.
[63] Cabral H, Nishiyama N, Kataoka K. Supramolecular nanodevices: from design validation to theranostic nanomedicine. Acc Chem Res 2011;44:999–1008.
[64] Saha K, Agasti SS, Kim C, et al. Gold nanoparticles in chemical and biological sensing. Chem Rev 2012;112:2739–79.
[65] Schuller JA, Barnard ES, Cai W, et al. Plasmonics for extreme light concentration and manipulation. Nat Mater 2010;9:193–204.
[66] Wax A, Sokolov K. Molecular imaging and darkfield microspectroscopy of live cells using gold plasmonic nanoparticles. Laser Photonics Rev 2009;3:146–58.
[67] Jin Y, Jia C, Huang SW, et al. Multifunctional nanoparticles as coupled contrast agents. Nat Commun 2010;1:41.
[68] Hu X, Wei CW, Xia J, et al. Trapping and photoacoustic detection of CTCs at the Single Cell per milliliter level with magneto-optical coupled nanoparticles. Small 2013;9:2046–52.
[69] Wang Y, Xu J, Wang Y, et al. Emerging chirality in nanoscience. Chem Soc Rev 2013;42:2930–62.
[70] He J, Wei Z, Wang L, et al. Hydrodynamically driven self-assembly of giant vesicles of metal nanoparticles for remote-controlled release. Angew Chem Int Ed Engl 2013;52:2463–8.
[71] Lin J, Wang S, Huang P, et al. Photosensitizer-loaded gold vesicles with strong plasmonic coupling effect for imaging-guided photothermal/photodynamic therapy. ACS Nano 2013;7:5320–9.
[72] Dreaden EC, Mackey MA, Huang X, et al. Beating cancer in multiple ways using nanogold. Chem Soc Rev 2011;40:3391–404.
[73] Wang Y, Wang K, Zhao J, et al. Multifunctional mesoporous silica-coated graphene nanosheet used for chemo-photothermal synergistic targeted therapy of glioma. J Am Chem Soc 2013;135:4799–804.
[74] Singh AK, Khan SA, Fan Z, et al. Development of a long-range surface-enhanced Raman spectroscopy ruler. J Am Chem Soc 2012;134:8662–9.
[75] Wang E, Desai MS, Lee SW. Light-controlled graphene-elastin composite hydrogel actuators. Nano Letters 2013;13:2826–30.
[76] Yuan H, Fales AM, Vo-Dinh T. TAT peptide-functionalized gold nanostars: enhanced intracellular delivery and efficient NIR photothermal therapy using ultralow irradiance. J Am Chem Soc 2012;134:11358–61.
[77] Beqa L, Fan Z, Singh AK, et al. Gold nano-popcorn attached SWCNT hybrid nanomaterial for targeted diagnosis and photothermal therapy of human breast cancer cells. ACS Appl Mater Interfaces 2011;3:3316–24.